DEUTSCHES ELEKTRONEN-SYNCHROTRON **DESY**

DESY 79/31
June 1979

EXPERIMENTAL RESULTS ON THE DECAY SEQUENCES $\psi'(3685) \to \gamma P_c/\chi \to \gamma\gamma J/\psi$, $\gamma\pi^+\pi^-$, γK^+K^- AND THE DECAYS $\psi' \to \eta J/\psi$, $\pi^0 J/\psi$

DASP Collaboration

NOTKESTRASSE 85 · 2 HAMBURG 52

To be sure that your preprints are promptly included in the
HIGH ENERGY PHYSICS INDEX ,
send them to the following address (if possible by air mail) :

DESY
Bibliothek
Notkestrasse 85
2 Hamburg 52
Germany

Experimental Results on the Decay Sequences $\psi'(3685) \to \gamma P_c/\chi \to \gamma\gamma J/\psi$, $\gamma\pi^+\pi^-$, γK^+K^- and the Decays $\psi' \to \eta J/\psi$, $\pi^0 J/\psi$

DASP Collaboration

R. Brandelik, W. Braunschweig, H.-U. Martyn, H.G. Sander, D. Schmitz, W. Sturm[1] and W. Wallraff
I. Physikalisches Institut der RWTH Aachen

D. Cords, R. Felst, R. Fries[9], E. Gadermann[1], H. Hultschig, P. Joos, W. Koch, U. Kötz, H. Krehbiel, D. Kreinick[2], H.L. Lynch, W.A. McNeely[3], G. Mikenberg[5], K.C. Moffeit[4], D. Notz, M. Schliwa, A. Shapira[5], B.H. Wiik and G. Wolf
Deutsches Elektronen-Synchrotron DESY, Hamburg

L. Ludwig[6], K.H. Mess[7], A. Petersen, G. Poelz, J. Ringel, O. Römer, R. Rüsch, K. Sauerberg and P. Schmüser
II. Institut für Experimentalphysik der Universität Hamburg

W. de Boer, G. Buschhorn, W. Fues, Ch. von Gagern, G. Grindhammer, B. Gunderson, R. Kotthaus, H. Lierl[3] and H. Oberlack
Max-Planck-Institut für Physik und Astrophysik, München

S. Orito, T. Suda[10], Y. Totsuka and S. Yamada
Lab. of Int. Coll. on Elementary Particle Physics and Department of Physics, University of Tokyo, Japan

Abstract:
In an analysis of the $\gamma\gamma\mu^+\mu^-$ final state observed in ψ' decays we investigate the radiative cascade transitions $\psi' \to \gamma P_c/\chi \to \gamma\gamma J/\psi$ and the decays $\psi' \to \eta J/\psi$, $\pi^0 J/\psi$. Furthermore, the decay sequences $\psi' \to \gamma\chi \to \gamma\pi^+\pi^-$, γK^+K^- are observed in a study of hadron pairs from ψ' decays. Decay branching ratios (or limits on them) are presented and compared to those from other experiments.

1) Now at Beiersdorf A.G., Hamburg
2) Now at Cornell University, USA
3) Now at Boeing Computer Services, Seattle, Washington, USA
4) Now at SLAC, USA
5) On leave from the Weizmann Institute, Rehovot, Israel
6) Now at California Institute of Technology, USA
7) Now at CERN
8) Now at University of Dortmund
9) Now at Northwestern University Evanston, Physics Deparment
10) Now at Cosmic Ray Lab., University of Tokyo, Japan

1. Introduction

Since the first experimental observation of intermediate $c\bar{c}$ P-wave states[1] predicted within the framework of the charmonium model[2,3,4,5] various groups have presented results on the radiative transitions between these states and the ψ' and J/ψ levels[6-13] or on hadronic decays of the P-wave states[12,14]. At present 3 such states with masses around 3.41, 3.51 and 3.55 GeV are firmly established[15]. The most likely spin-parity C-parity assignments are 0^{++}, 1^{++} and 2^{++}, respectively, corresponding to the states $^3P_0$, $^3P_1$, $^3P_2$ in the charmonium level scheme. The existence of a fourth intermediate state with mass 3.45 GeV is less evident[11-13]. It had been considered as a candidate for the first radially excited level of the $^1S_0$ charmonium state, although its low lying mass and the apparent absence of hadronic decays causes theoretical difficulties[16]. Recently it has obtained competition in this role from a new state at a mass around 3.59 GeV, for which evidence was claimed by the DESY-Heidelberg collaboration[13].

On several occasions our collaboration has reported results on the radiative cascade decays[17]

$$\psi' \rightarrow \gamma P_c/\chi \qquad (1a)$$

$$P_c/\chi \rightarrow \gamma J/\psi \qquad (1b)$$

where P_c/χ denotes the P_c state with a mass of 3.51 GeV and the χ states seen at 3.41 and 3.55 GeV, respectively. In this paper we present our final results on the product of branching ratios for the decays (1a),(1b)[18]. In the same analysis we also obtain a value for the decay branching ratio of

$$\psi' \rightarrow \eta J/\psi \qquad (2)$$

and an upper limit for the branching ratio of the decay

$$\psi' \rightarrow \pi^0 J/\psi \qquad (3)$$

which violates I-spin conservation.

As a by-product of a search for ψ' decays into hadron pairs we observe the decay sequences $\psi' \rightarrow \gamma\chi \rightarrow \gamma\pi^+\pi^-$, γK^+K^- and present results on their products of branching ratios.

2. Apparatus

The DASP detector[19] operating at the e^+e^- storage ring DORIS consists of two identical magnetic spectrometer arms of opposite orientation normal to the beam line (see Figs. 1, 2). Each arm contains 6 planes of proportional wire chambers next to the beam pipe, 2 planes of magnetostrictive wire chambers before and 10 planes behind the magnet, an array of time of flight counters and lead sandwich shower counters at a distance of ~5 m from the interaction point. Scintillation counters behind a 70 cm thick iron filter ("range counters") serve to identify muons. The geometric acceptance of both spectrometer arms is 7% of 4π, the momentum resolution in this experiment is $\sigma_p/p = 1\ \%\ p/GeV$, and the angular resolution of charged particles traversing the proportional chambers is $\Delta\Theta \approx \Delta\Phi \approx 6$ mr. Furthermore there are two Cerenkov counters covering the magnet aperture for better electron identification. A nonmagnetic inner detector filling the space between beam pipe and magnet covers 70 % of the full solid angle. It serves the detection of charged tracks and γ rays. A particle leaving the interaction point within the acceptance of the inner detector will hit successively 4 sandwich detectors, each consisting of a layer of scintillators, a lead sheet ($1\ X_0$) and 2 or 3 layers of proportional tube chambers, and will then penetrate into a lead sandwich shower counter ($7\ X_0$). The direction of γ rays in the inner detector is determined with an accuracy of 16 to 45 mrad, depending on the direction of the particle. The detection efficiency of photons in the inner detector rises from 50 % at 50 MeV photon energy to 80 % at 100 MeV and is more than 95 % above 250 MeV. The γ energy resolution is $\sigma_E/E = 17\ \%/\sqrt{E/GeV}$.

3. Analysis of the $\gamma\gamma\mu^+\mu^-$ final state

This analysis is based on 304000 observed events which have been taken at energies around the centre of the ψ' resonance. They correspond to an integrated luminosity of 1460 nb^{-1}.

Reactions (1), (2) and (3) were searched for in ψ' decays leading to a $\mu^+\mu^-$ final state:

$$\psi' \rightarrow \gamma\ \gamma\ J/\psi \qquad J/\psi \rightarrow \mu^+\mu^- \tag{4}$$

In order to select events with a μ pair we start the analysis considering two event classes.

In class 1 we select events where two charged particles of opposite charge had to traverse the magnet arms with momenta between 1.1 and 2.2 GeV. To discriminate against electrons, the energy per track deposited in the shower counters had to be less than 450 MeV. (The average energy deposited by a minimum ionizing particle was 80 MeV.) Traversal of the iron filter, i.e. a clear muon signature, was not required for this event class, since such a requirement would have introduced an unnecessary cut in the geometric acceptance.

In class 2 we consider events with only one charged particle detected in the magnetic spectrometer. This particle had to have a momentum between 1.1 and 2.2 GeV and had to be identified as muon by a signal in the scintillation counters behind the iron filter and by pulse height in the shower counters. Furthermore, at least one other charged track had to be observed in the inner detector (outside the acceptance of the spectrometers) and had to form an angle between 150^0 and 180^0 with the identified muon track.

In Fig. 3 we show for class 1 events the invariant mass distribution of the two charged tracks traversing the magnet having assigned to them the muon mass. The ψ' and J/ψ resonances are clearly visible.

Fig. 4a shows the momentum distribution of the charged tracks in class 1 events. The peaks around 1.8 GeV and 1.5 GeV correspond to the ψ' and J/ψ decays, respectively. To this we compare in Fig. 4b the momentum spectrum of the single muon of class 2 events. The shape of this spectrum agrees with the lower part of the spectrum of class 1 events and shows that class 2 events predominantly arise from J/ψ decay. ($\psi' \rightarrow \mu\mu$ decays and μ pairs from QED which give rise to the peak at 1.8 GeV in Fig. 4a enter only into class 1 because of their collinear decay configuration.)

There were 1130 events of class 1 where a 1C fit to the J/ψ mass gave a $\chi^2 < 10$. Those and all 706 class 2 events entered the further analysis. About 80 % of these events had other tracks, charged or neutral, in the inner detector. A unique determination of the number of charged and neutral tracks in an event was not always possible on the basis of our track reconstruction programs alone. The computer programs would rarely lose a track, in more complicated cases, however, they showed a tendency to interprete spray from showers as independent tracks. As a consequence visual inspection of the event display was necessary. In order to reduce the number of events to be inspected the following preselection was done by computer. If at least one neutral track was found in the inner

detector, all tracks except the muon tracks were assigned to photons and a kinematic fit to reaction (4) was tried for all $\gamma\gamma$ combinations. Considering the γ energies as unmeasured this was a 3C fit for class 1 events and a 2C fit for class 2. Events giving at least one fit with $\chi^2 < 20$ were inspected by physicists in order to eliminate cases with not exactly two γ's and two charged tracks. After this procedure we were left with 65 events of class 1 and 56 of class 2. Their χ^2 probability for the kinematic fits is shown in Fig. 5a,b. The peaks for probability < 0.05 signal the presence of background events. Since the fit of μ pairs to the J/ψ mass had given a flat probability distribution (not shown) we have to conclude that the slow increase of the distributions in Fig. 5a,b towards higher probability indicates an overestimate of the errors in the measured γ direction.

83 events with a χ^2 probability greater than 0.14 entered the physics analysis of the $\gamma\gamma$ J/ψ final state.

4. Interpretation of the invariant mass spectra

In Fig. 6 we plot the higher value of the two possible $\gamma J/\psi$ invariant mass combinations versus the $\gamma\gamma$ invariant mass. The accumulation of events around $m_{\gamma\gamma} = 550$ MeV is due to the decay $\psi' \to \eta J/\psi$. The width of this peak agrees with the expected η mass resolution of $\sigma_M = 10$ MeV. There is no clear indication of a $\psi' \to \pi^0 J/\psi$ decay. The remaining events can be explained as arising from intermediate P_c/χ states according to the decay sequence (1a), (1b) and from background predominantly due to the reaction

$$\psi' \to \pi^0\pi^0 J/\psi \qquad (5)$$

where two γ's in the final state escape detection.

Removing η events with invariant $\gamma\gamma$ masses above 520 MeV we plot in Fig. 7 the low $\gamma J/\psi$ invariant mass combination versus the high one. The projection onto the axis of high invariant mass (Fig. 8a) reveals several event clusters, whereas the projection onto the other axis (Fig. 8b) shows rather a broad bump.

The only nonnegligible background to the $\gamma\gamma\mu^+\mu^-$ final state originates from reaction (5). We have calculated this background with Monte Carlo techniques assuming a branching ratio for $\psi' \to \pi^0\pi^0 J/\psi$ of 17 %[20] and an S wave decay of the ψ' into J/ψ plus a spin 0 ε-resonance. The parametrization of the generated $\pi^0\pi^0$ mass distribution was taken from ref. 21, the resonance mass and width

were determined by a fit to the spectrum of the missing mass conjugate to the J/ψ as discussed in section 6. The result of this calculation is shown as broken line in Fig. 8. The peaks in the invariant mass spectrum at 3.51 and 3.55 GeV are clear evidence for the $P_c(3.51)$ and $\chi(3.55)$ states. Less clear is the interpretation of the event clusters at 3.45 GeV and 3.40 GeV. In this analysis they are compatible with the expected background. While the $\chi(3.41)$ state is well established through its hadronic decays (see refs. 12,14, also section 8) the possible state at 3.45 GeV has been observed in the $\gamma J/\psi$ decay mode only and the evidence for its existence is not overwhelming[12,15]. In fact in a recent analysis of the DESY-Heidelberg group[13] no positive evidence is found for this state. On the other hand this group has reported evidence for a new state at a mass of 3.59 GeV (or 3.18 GeV); in our analysis the 3 events above 3.58 GeV are consistent with such a state. We expect 2 events on the basis of the reported value of $(0.18 \pm 0.06) \cdot 10^{-2}$ for the product of branching ratios of the $\psi' \to \gamma\gamma J/\psi$ decay via this state. However it cannot be excluded that those 3 events belong to the cluster at 3.55 GeV due to a non-Gaussian tail in the γ angular resolution.

To the observed invariant mass spectrum above 3.43 GeV we have fitted the sum of 2 Gaussian resolution functions plus the calculated background term. In this fit only the masses and intensities of the 3.51 and 3.55 GeV states were treated as free parameters, the variances of the Gaussians had been obtained by Monte Carlo calculation: σ = 10 MeV for 3C fits, 13 MeV for 2C fits and 11 MeV for the sum of both. Shape and magnitude of the background were inserted without free parameter into the fit. As a result we obtained the masses of the two higher lying states to be 3.509 ±0.011 GeV and 3.551 ±0.011 GeV, respectively, in good agreement with the corresponding world averages[15], 3.508 ±0.004 GeV and 3.554 ±0.005 GeV. From the fitted intensities corresponding decay branching ratios were obtained as discussed in the next section.

5. Branching ratios of cascade decays

Branching ratios of ψ' decays leading to a J/ψ plus a particle system S in the final state were determined using the relation

$$B(\psi' \to SJ/\psi) = \frac{\Gamma(\psi' \to SJ/\psi)}{\Gamma(\psi' \to \text{all})} = \frac{N_{prod}(\psi' \to SJ/\psi,\ J/\psi \to \mu^+\mu^-)}{N_{prod}(\psi' \to \text{all})} \cdot \frac{1}{B(J/\psi \to \mu^+\mu^-)}. \qquad (6)$$

Here N_{prod} denotes the number of produced events in the experiment and the factor $1/B(J/\psi \to \mu^+\mu^-)$ corrects for the fact that the J/ψ is observed in the $\mu^+\mu^-$ decay mode. N_{prod} is connected to N_{obs}, the observed number of events, by the relation

$$N_{prod} = N_{obs}/\varepsilon \qquad (7)$$

where ε is the detection efficiency of a particular decay mode depending on the geometry of the detector, the performance of the detector components, analysis losses, and also on the dynamics of the decay process which affects momenta and angular correlations of the particles in the final state. The detection efficiencies for the various final states studied were obtained by Monte Carlo simulation of the experiment.

The data treated in the analysis are normalized to a total of $N_{obs}(\psi' \to all) = 304\,000$ observed ψ' events (after background subtraction) whose overall detection efficiency was determined to be $\varepsilon(\psi' \to all) = 0.35$ by a method completely analogous to that employed by us in the determination of the total hadronic e^+e^- cross section outside the J/ψ and ψ' [22].

For the branching ratio $B(J/\psi \to \mu^+\mu^-)$ appearing in relation (6) we used the value (7.6 ±1.1) % as obtained from our analysis of J/ψ decays [23].

When calculating detection efficiencies for the P_c/χ states we assumed the spin parity assignments 0^+, 1^+, 2^+ for the $\chi(3.41)$, $P_c(3.51)$ and $\chi(3.55)$ which are suggested by theory and by experimental findings [12]. While angular momentum conservation fixes completely the cascade decay via the 0^+ state (E1 emission of both successive γ's), the decays via the 1^+ and 2^+ state admit 2 or 3 multipoles, respectively. Only the lowest multipole (E1) was assumed to contribute, as suggested from theoretical arguments[25]. In the acceptance calculation the full angular (and momentum) correlations of the three successive decays were taken into account. Those correlations are given for instance in references 24) and 25).

Table I shows our results on the radiative cascade decay branching ratios. Also listed are the fitted masses of the $P_c(3.51)$ and $\chi(3.55)$ and the observed numbers of events from which the branching ratios were derived. The errors quoted are statistical only. The systematic error for the branching ratios is of the order of 20 %. Within the quoted errors there is agreement between our results on the branching ratios and those obtained in other experiments as can be seen from a comparison presented in Table III.

6. Branching ratio for $\psi' \to \eta\, J/\psi$

The number of observed η's is readily obtained from Fig. 6b when fitting a Gaussian resolution function for the η mass plus the calculated shape of background contribution from P_c/χ and $\pi^o\pi^o J/\psi$ states to the observed $\gamma\gamma$ mass spectrum. 16.9 ±4.3 η events above background lead to a branching ratio $B(\psi' \to \eta J/\psi)$ = (3.5 ±0.9) %.

Another method to determine this branching ratio is based on a fit to the spectrum of missing masses recoiling from the J/ψ in class 1 events. This type of analysis leads to different systematic uncertainties compared to the first one. Fig. 9 shows this spectrum calculated after the observed muon momentum vectors had been fitted to the mass of the J/ψ. The spectrum peaks at the η mass. A sum of 3 terms was fitted to this distribution: The first term describes the contribution from ψ' decays via intermediate P_c/χ states. It was obtained by Monte Carlo simulation of the experiment and entered into the fit without free parameters. The second term is meant to describe the majority of $\psi' \to J/\psi + X$ decays. Since ~ 85 % of all cascade decays lead to a $\pi\pi J/\psi$ final state a parametrization suited to describe the $\pi\pi$ invariant mass distribution seems adequate. We use the parametrization suggested by J. Schwinger et al.[21] in terms of a scalar isoscalar ε resonance, folded with the acceptance of μ pairs from the subsequent J/ψ decay. Finally the 3rd term is a Gaussian resolution function for the η mass with σ obtained from Monte Carlo studies.

In a first fit, cutting out of the η mass region, the shape of the background was determined in terms of mass and width of the ε resonance yielding m_ε = 710 ±70 MeV, Γ_ε = 910 ±110 MeV. We consider these values only as a suitable background description and not as a measurement of the ε resonance parameters. In a second fit, keeping the shape of the background constant, the magnitude of the η signal was found to be 97 ±20 events from which a branching ratio of (3.5 ±0.7) % was deduced, in agreement with that obtained from direct η observation. The error on the $\psi' \to \eta J/\psi$ branching ratio obtained from the missing mass spectrum has to be considered with some caution since it largely depends on the details of the background parametrization.

The comparison in Table III shows good agreement between our result and those of other experiments.

7. Limit on the branching ratio $\psi' \to \pi^0 J/\psi$

In all events fitting the hypothesis $\psi' \to \gamma\gamma\ J/\psi$, $J/\psi \to \mu^+\mu^-$ the invariant $\gamma\gamma$ mass has been constrained to the π^0 mass yielding 4C and 3C kinematic fits for class 1 and class 2 events, respectively. Fig. 10a shows the χ^2 distribution of these fits. Two events of class 1 and 8 events of class 2, all having χ^2's smaller than 8, were considered as candidates for the decay $\psi' \to \pi^0\ J/\psi$. In Fig. 10b the $\gamma\gamma$ opening angle distribution for the 10 candidates is plotted. The dashed line shows the expected $\gamma\gamma$ opening angle distribution for $\psi' \to \pi^0 J/\psi$ normalized to the 10 candidates. It peaks at 30^0. Also shown as dashed-dotted line is the corresponding distribution expected for radiative cascade decays normalized to 38 observed events. It is essentially flat. The observed distribution is flat, too, and we have to assume that our 10 π^0 candidates are just the expected background from radiative decays. The upper limit for the branching ratio of the I-spin forbidden decay $\psi' \to \pi^0\ J/\psi$ is calculated to be

$$B(\psi' \to \pi^0\ J/\psi) \ < \ 0.4\ \%\ (90\ \%\ \text{c.l.}),$$

well compatible with the range of theoretical predictions ($0.04\% \leq B \leq 0.3\%$), which relate this decay to the $\psi' \to \eta\ J/\psi$ decay assuming an isospin violating $\eta \to \pi^0$ transition[29]. Somewhat lower experimental limits have been reported by refs. 13 and 26. They are listed in Table III.

8. The decay sequences $\psi' \to \gamma\chi \to \gamma\pi^+\pi^-$, γK^+K^-

These decays have been observed in a different analysis studying hadron pairs from ψ' decays[27]. The following criteria have been applied in order to select hadron pair candidates. Two charged tracks of opposite sign were required to traverse the magnet arms within the solid angle covered by the range counter. Assigning the pion mass to these tracks they had to form an invariant mass larger than 2.8 GeV and the missing mass conjugate to the pair had to be samller than 0.5 GeV. Neither of the tracks was allowed to cause a signal in the range counters which leads to a μ-pair rejection factor of $> 10^3$. In order to discriminate against electron pairs we made use of the information given by the two Cerenkov counters covering the magnet apertures or by the shower counters behind the magnets. An electron pair rejection factor of $> 3 \cdot 10^3$ was reached. In the range of particle momenta considered in this analysis only marginal π/K separation is possible by time of flight criteria. Protons, however, can be completely separated from π's and K's by the time of flight measurement. After having cut out $p\bar{p}$ events we were left with 49 π or K pair candidates. By kinematics 5

of those events are consistent with hadronic two-body decays, 3 of which are examples of the decay $\psi \to \pi^+\pi^-$ and 2 of $\psi' \to K^+K^-$.

The remaining 44 events have been fitted to the hypotheses $\psi' \to \gamma\,\pi^+\pi^-$, γK^+K^-. If an accompanying γ had been observed in the inner detector a 4C fit was tried, otherwise a 1C fit. The γ energy measured in the inner detector with an error of $\sigma_E/E = 17\ \% / \sqrt{E/\mathrm{GeV}}$ was used as measured variable in the 4C fits.

Fig. 11 shows the χ^2 probability distribution of both 1C and 4C fits always selecting the hypothesis with the higher probability. The invariant hadron pair mass of events with a χ^2 probability > 2 % is plotted in Fig. 12. There are 32 entries in this plot, 11 corresponding to 4C fits and 21 to 1C fits. If both hypotheses, $\gamma\pi^+\pi^-$ and γK^+K^-, gave an acceptable χ^2 only the hypothesis with the larger probability entered the plot; γK^+K^- events appear as shaded area. A Monte Carlo simulation has shown that this procedure will pick out the correct hypothesis in 96 % of the cases. Usually the hadron mass assignment resulting from the fit agrees with that favoured by the time of flight measurement.

The invariant mass plot of Fig. 12 reveals two event accumulations, one at a mass of 3.41 GeV which we attribute to the $\pi^+\pi^-$, K^+K^- decay of the $\chi(3.41)$ state, and another one at 3.55 GeV, which is apparently caused by the corresponding $\chi(3.55)$ decay. The observed widths of these peaks agree with the expected mass resolution of σ_M = 20 MeV. There are no events observed in the mass region of the $P_c(3.51)$ in accordance with its favoured spin parity assignment 1^+ which would forbid the decay into pairs of spin 0 bosons.

In the region below the $\chi(3.41)$ mass 8 events are observed. They must be of hadronic origin, since we expect altogether less than one event from γe^+e^-, $\gamma\mu^+\mu^-$ final states. Possible sources for these events are the decays $\psi' \to \pi^+\pi^-\pi^0$, $K^+K^-\pi^0$ with none or only one γ observed, arising from the decay of a slow π^0. A Monte Carlo study shows that background from these sources has a rather flat invariant mass distribution between 3 GeV and 3.3 GeV from where it gradually drops to zero at ~ 3.6 GeV. The tail of low masses observed experimentally is, qualitatively, not inconsistent with the assumption of such a background source. A quantitative statement is not possible, since branching ratios for those decays are unknwon. In any case, background from 3- or more-body hadronic ψ' decays cannot produce peaks at masses between 3.4 and 3.6 GeV unless the final state contains a resonance in this mass interval. In the calculation of branching ratios one $\gamma\pi\pi$ event in the cluster around 3.41 GeV was subtracted as background.

Among 19 proton pair candidates 4 proved to be examples of the decay $\psi' \to p\bar{p}$. Of the remaining 15 events there was none fitting the hypothesis $\psi' \to \gamma p\bar{p}$.

In Table II we present our results on the product of branching ratios for the subsequent decays $\psi' \to \gamma\chi$, $\chi \to \pi^+\pi^-$, K^+K^-, $p\bar{p}$. In the acceptance calculation again the full angular correlations of all decay products were taken into account assuming the first decay to proceed via an electric dipole transition and assigning spin 0 to the $\chi(3.41)$ and spin 2 to $\chi(3.55)$. The $\chi \to p\bar{p}$ decay was assumed to be isotropic. Our results on the decay sequences $\psi' \to \gamma\chi \to \gamma\pi^+\pi^-$, γK^+K^- are consistent with those obtained by the SLAC-LBL collaboration[12,26]; see Table III for comparison.

9. Summary and comparison to other experiments

In summary we have determined products of branching ratios for successive radiative cascade decays of the type $\psi' \to \gamma P_c/\chi \to \gamma\gamma J/\psi$. There is no evidence for the existence of a state at 3.45 GeV in our data. We can only give an upper limit for the successive decay branching ratio via such a state. Furthermore, in a different analysis, values for the branching ratio products of the decay sequences $\psi \to \gamma\chi \to \gamma\pi^+\pi^-$, γK^+K^- have been obtained. We also present our value for the branching ratio of the decay $\psi' \to \eta J/\psi$ and quote an upper limit for the $\psi' \to \pi^0 J/\psi$ branching ratio.

In Table III our results are compared to those obtained by other experiments. There is overall agreement within the experimental errors.
It has to be noted that the errors quoted in our results are statistical only and that we cannot exclude an additional systematic error of 20% which is mainly due to the uncertainty in the number of produced ψ' states and in $B(J/\psi \to \mu^+\mu^-)$.

Acknowledgements

We would like to thank the engineers and technicians from DESY and the collaborating institutions who have made this experiment possible by building, operating and maintaining DESY, DORIS, DASP and the computer centre. The non-DESY members of the collaboration thank the DESY directorate for their hospitality.

References:

1) W.Braunschweig et al., Phys.Lett. 57B, 407 (1975)

2) T.Appelquist and H.D.Politzer, Phys.Rev.Lett. 34, 46 (1975)
T.Appelquist et al., ibid. 34, 365 (1975)

3) M.K.Gaillard, B.W.Lee, and J.L.Rosner, Rev.Mod.Phys. 47, 277 (1975)

4) C.G.Callan et al., Phys.Rev.Lett. 34, 52 (1975)

5) E.Eichten et al., Phys.Rev.Lett. 34, 369 (1975)

6) W.Tanenbaum et al., Phys.Rev.Lett. 35, 1323 (1975)

7) J.S.Whitaker et al., Phys.Rev.Lett. 37, 1596 (1976)

8) H.Rieseberg, invited talk on results from the DESY-Heidelberg Collaboration, in Particle Searches and Discoveries - 1976 proceedings of the Second International Conference in High Energy Physics at Vanderbilt University, edited by R.S. Panvini (AIP, New York 1976), p. 274

9) J.E.Olsson, DESY-Heidelberg-Collaboration, Proc. of the 8th Intern. Symposium on Lepton and Photon Interactions at High Energies, Hamburg, 1977 and DESY 77/70 (1977)

10) C.J.Biddick et al., Phys.Rev.Lett. 38, 1324 (1977)

11) V.Blobel, "Recent Results on e^+e^- Annihilation from PLUTO at DORIS", Proceedings of the 12^{th} Rencontre de Moriond 1977, Vol. I, p. 99

12) W.Tanenbaum et al., Phys.Rev. D 17, 1731 (1978)

13) W.Bartel et al., Phys. Lett. 97B, 492 (1978)

14) G.J.Feldman et al., Phys.Rev. Lett. 35, 821 (1975)

15) Review of Particle Properties, Particle Data Group, Physics Lett. 75B (1978)

16) M.S.Chanowitz and F.J.Gilman, Phys.Lett. 63B, 178 (1976)

17) e.g. B.H.Wiik, Proceedings of the 1975 International Symposium on Lepton and Photon Interactions at High Energies p. 69, and S.Yamada, Proceedings 1977 International Symposium on Lepton and Photon Interactions at High Energies p. 69

18) For a more detailed description of the analysis we refer to E.Gadermann, thesis, Interner Bericht DESY F22-78/05

19) More detailed descriptions of the DASP detector can be found in W.Braunschweig at al., Phys.Lett. 56B, 491 (1975) ibid. 67B, 243 (1977)

20) G.S.Abrams et al., Phys.Rev.Lett. 37, 1181 (1975) and ref. 14.

21) J.Schwinger et al., Phys.Rev. D12, 2617 (1975)

22) R.Brandelik et al., Phys.Lett. 76B, 361 (1978)

23) K.Sauerberg, thesis 1979, University Hamburg , also R. Brandelik et al., Z. Physik C, 1, 233 (1979)

24) L.S.Brown, R.M.Cahn, Phys.Rev. D13, 1195 (1976)

25) G.Karl, S.Meshkov, J.L.Rosner, Phys.Rev. D 13, 1203 (1976)

26) W. Tanenbaum et al., Phys.Rev.Lett. 36, 402 (1976)

27) M. Schliwa, thesis 1979, University Hamburg

28) A. M. Boyarski et al. Phys. Rev. Lett. 34, 1357 (1975)

29) G. Segrè and J. Weyers, Phys. Lett. 62B, 91 (1976)

Table I: Branching ratios for ψ' decays studied in the $\gamma\gamma\mu^+\mu^-$ final state

ψ' decay mode	Mass of intermediate state in GeV	Number of observed events above background	Branching ratios
			$B(\psi' \to \gamma P_c/\chi) \cdot B(P_c/\chi \to \gamma J/\psi)$
$\psi' \to \gamma P_c/\chi$	3.413 ± 0.005 [15]	2.4 ± 1.9	$(0.3 \pm 0.2) \cdot 10^{-2}$
	$3\,454 \pm 0.010$ [15]	< 4.5 (90 % c.l.)	$< 0.4 \cdot 10^{-2}$ (90% c.l.)
$\hookrightarrow \gamma J/\psi$	3.509 ± 0.011	20.6 ± 4.5	$(1.7 \pm 0.4) \cdot 10^{-2}$
	3.551 ± 0.011	14.9 ± 3.9	$(1.4 \pm 0.4) \cdot 10^{-2}$
			$B(\psi' \to fJ/\psi)$
$\psi' \to \eta J/\psi$	-	16.9 ± 4.3	$(3.5 \pm 0.9) \cdot 10^{-2}$
$\psi' \to \pi^0 J/\psi$	-	< 5.5 (90 % c.l.)	$< 0.4 \cdot 10^{-2}$ (90% c.l.)

Table II: Branching ratios for ψ' decays studied in $\gamma\pi^+\pi^-$, γK^+K^-, $\gamma p\bar{p}$ final states

ψ' decay mode	Number of observed events above background	Product of branching ratios $B(\psi' \to \gamma P_c/\chi) \cdot B(P_c/\chi \to f)$
$\psi' \to \gamma\chi(3.41)$		
$\quad \hookrightarrow \pi^+\pi^-$	11	$(5.9 \pm 2.1) \cdot 10^{-4}$
$\quad \hookrightarrow K^+K^-$	6	$(5.4 \pm 2.5) \cdot 10^{-4}$
$\quad \hookrightarrow p\bar{p}$	0	$< 0.94 \cdot 10^{-4}$ (90% c.l.)
$\psi' \to \gamma P_c(3.51)$		
$\quad \hookrightarrow \pi^+\pi^-$ *)	0	$< 1.2 \cdot 10^{-4}$ (90% c.l.)
$\quad \hookrightarrow K^+K^-$ *)	0	$< 2.1 \cdot 10^{-4}$ (90% c.l.)
$\quad \hookrightarrow p\bar{p}$	0	$< 1.0 \cdot 10^{-4}$ (90% c.l.)
$\psi \to \gamma\chi(3.55)$		
$\quad \hookrightarrow \pi^+\pi^-$	4	$(1.5 \pm 0.8) \cdot 10^{-4}$
$\quad \hookrightarrow K^+K^-$	2	$(1.2 \pm 0.9) \cdot 10^{-4}$
$\quad \hookrightarrow p\bar{p}$	0	$< 0.74 \cdot 10^{-4}$ (90% c.l.)

*) assuming $P_c(3.51)$ to be a $J^{PC} = 0^{++}$ state

Table III: Branching ratios of ψ' decays. Results from different experiments

ψ' decay mode	DASP	DESY-Heidelberg [13]	MPSSD [10]	SLAC-LBL [12,26]
	Products of branching ratios: $B(\psi' \to \gamma P_c/\chi) \cdot B(P_c/\chi \to f)$			
$\psi' \to \gamma\chi(3.41)$				
$\hookrightarrow \gamma J/\psi$	$(0.3 \pm 0.2) \cdot 10^{-2}$	$(0.14 \pm 0.09) \cdot 10^{-2}$	$(3.3 \pm 1.7) \cdot 10^{-2}$	$(0.2 \pm 0.2) \cdot 10^{-2}$
$\hookrightarrow \pi^+\pi^-$	$(5.9 \pm 2.1) \cdot 10^{-4}$	-	-	$(7.5 \pm 2.1) \cdot 10^{-4}$
$\hookrightarrow K^+K^-$	$(5.4 \pm 2.5) \cdot 10^{-4}$	-	-	$(7.8 \pm 2.3) \cdot 10^{-4}$
$\hookrightarrow p\bar{p}$	$< 0.84 \cdot 10^{-4}$ (90%c.l.)	-	-	-
$\psi' \to \gamma\chi(3.45)$				
$\hookrightarrow \gamma J/\psi$	$< 0.4 \cdot 10^{-2}$ (90%c.l.)	$< 0.25 \cdot 10^{-2}$ (90%c.l.)	$< 2.5 \cdot 10^{-2}$ (90%c.l.)	$(0.8 \pm 0.4) \cdot 10^{-2}$
$\psi' \to \gamma P_c(3.51)$				
$\hookrightarrow \gamma J/\psi$	$(1.7 \pm 0.4) \cdot 10^{-2}$	$(2.5 \pm 0.4) \cdot 10^{-2}$	$(5.0 \pm 1.5) \cdot 10^{-2}$	$(2.4 \pm 0.8) \cdot 10^{-2}$
$\hookrightarrow \pi^+\pi^-$ *)	$< 1.2 \cdot 10^{-4}$ (90%c.l.)	-	-	-
$\hookrightarrow K^+K^-$ *)	$< 2.1 \cdot 10^{-4}$ (90%c.l.)	-	-	-
$\hookrightarrow p\bar{p}$	$< 1.0 \cdot 10^{-4}$ (90%c.l.)	-	-	-
$\psi' \to \gamma\chi$ (3.55)				
$\hookrightarrow \gamma J/\psi$	$(1.4 \pm 0.4) \cdot 10^{-2}$	$(1.0 \pm 0.2) \cdot 10^{-2}$	$(2.2 \pm 1.0) \cdot 10^{-2}$	$(1.0 \pm 0.6) \cdot 10^{-2}$
$\hookrightarrow \pi^+\pi^-$	$(1.5 \pm 0.8) \cdot 10^{-4}$	-	-	$(1.9 \pm 0.8) \cdot 10^{-4}$
$\hookrightarrow K^+K^-$	$(1.2 \pm 0.9) \cdot 10^{-4}$	-	-	
$\hookrightarrow p\bar{p}$	$< 0.74 \cdot 10^{-4}$ (90%c.l.)	-	-	-
	Branching ratios: $B(\psi' \to f J/\psi)$			
$\psi' \to \eta J/\psi$	$(3.5 \pm 0.9) \cdot 10^{-2}$	$(3.6 \pm 0.5) \cdot 10^{-2}$	-	$(4.3 \pm 0.8) \cdot 10^{-2}$
$\psi' \to \pi^0 J/\psi$	$< 0.4 \cdot 10^{-2}$ (90% c.l.)	$< 0.1 \cdot 10^{-2}$ (90%c.l.)	-	$< 0.15 \cdot 10^{-2}$ (90 % c.l.)

*) assuming $P_c(3.51)$ to be a $J^{PC} = 0^{++}$ state

Figure Captions:

Fig. 1 Schematic view of the DASP detector seen from above

Fig. 2 Schematic view of the DASP inner detector seen along the beam line

Fig. 3 Distribution of the invariant mass formed by two non-showering charged particles traversing the magnets with momenta between 1.1 GeV and 2.2 GeV. The particles were interpreted as muons, although there is some background from hadronic events.

Fig. 4 Muon momentum distributions:

a) for events with two muon (or hadron) tracks traversing the magnets. 1.1 GeV $\leq p \leq$ 2.2 GeV is required (class 1)

b) for events with one identified muon with momentum between 1.1 GeV and 2.2 GeV. Another charged track outside the magnet aperture is required, forming an angle between 150^{o} and 180^{o} with the identified muon (class 2)

Fig. 5 χ^2 probability distribution for kinematic fits to the reaction $\psi' \to \gamma\gamma\ J/\psi \to \gamma\gamma\ \mu^+\mu^-$; only events with $\chi^2 < 20$ enter.

a) 3C fits for events with two completely measured muon tracks and two γ rays with measured angles and unknwon momenta (class 1)

b) 2C fits for events with one completely measured muon and only angle measurements for the other tracks (class 2)

Fig. 6

a) The higher of the two possible $\gamma J/\psi$ invariant masses is plotted versus the invariant $\gamma\gamma$ mass. ● : 3C fit events, □ : 2C fit events.

b) Projection of a) onto the $M(\gamma\gamma)$ axis. Broken line: expected contribution from $\gamma P_c/\chi$ and $\pi^o\pi^o J/\psi$ states. Full line: fitted contribution from the $\eta J/\psi$ state.

Fig. 7 Distributions of invariant $\gamma J/\psi$ masses for fitted events with $M_{\gamma\gamma} < 520$ MeV. The lower $\gamma J/\psi$ invariant mass combination is plotted versus tne higher one. ● : 3C fits, □ : 2C fits

Fig. 8 Projections of the two-dimensional plot in Fig. 7.

a) Distribution of the higher $\gamma J/\psi$ invariant mass. Hatched area corresponds to class 1 events (3C fits). The full line is the result of a fit to the mass spectrum as described in the text. The broken line represents the background from $\psi' \to \pi^0\pi^0 J/\psi$ events

b) Distribution of the lower $\gamma J/\psi$ invariant mass. Meaning of hatched area and broken line as in 8a. The full line is the mass distribution expected from the results of the analysis

Fig. 9 Spectrum of missing masses recoiling from the J/ψ in class 1 events. The full line (η contribution) and dashed-dotted line ($\pi\pi$ contribution) are the result of a fit as described in the text. The broken line indicates the contribution from cascade decays via P_c/χ intermediate states.

Fig. 10 a) χ^2 distribution for 4C and 3C kinematic fits to the hypothesis $\psi' \to \pi^0 J/\psi$, $J/\psi \to \mu^+\mu^-$ for class 1 and class 2 events, respectively

b) Distribution of $\gamma\gamma$ opening angles of events with $\chi^2 < 8$.
Dashed line: Expectation for $\psi' \to \pi^0 J/\psi$ normalized to 10 events
Dashed-dotted line: Expectation for radiative cascade decays, normalized to 39 observed events.

Fig. 11 χ^2 probability distribution of 1C or 4C fits for events fitting one of the hypotheses $\psi' \to \gamma\pi^+\pi^-$, γK^+K^-.

Fig. 12 Distribution of $\pi^+\pi^-$ and K^+K^- (shaded area) invariant masses of events fitting the hypotheses $\psi' \to \gamma\pi^+\pi^-$, K^+K^- either with 4 constraints (measured γ) or 1 constraint (unobserved γ).

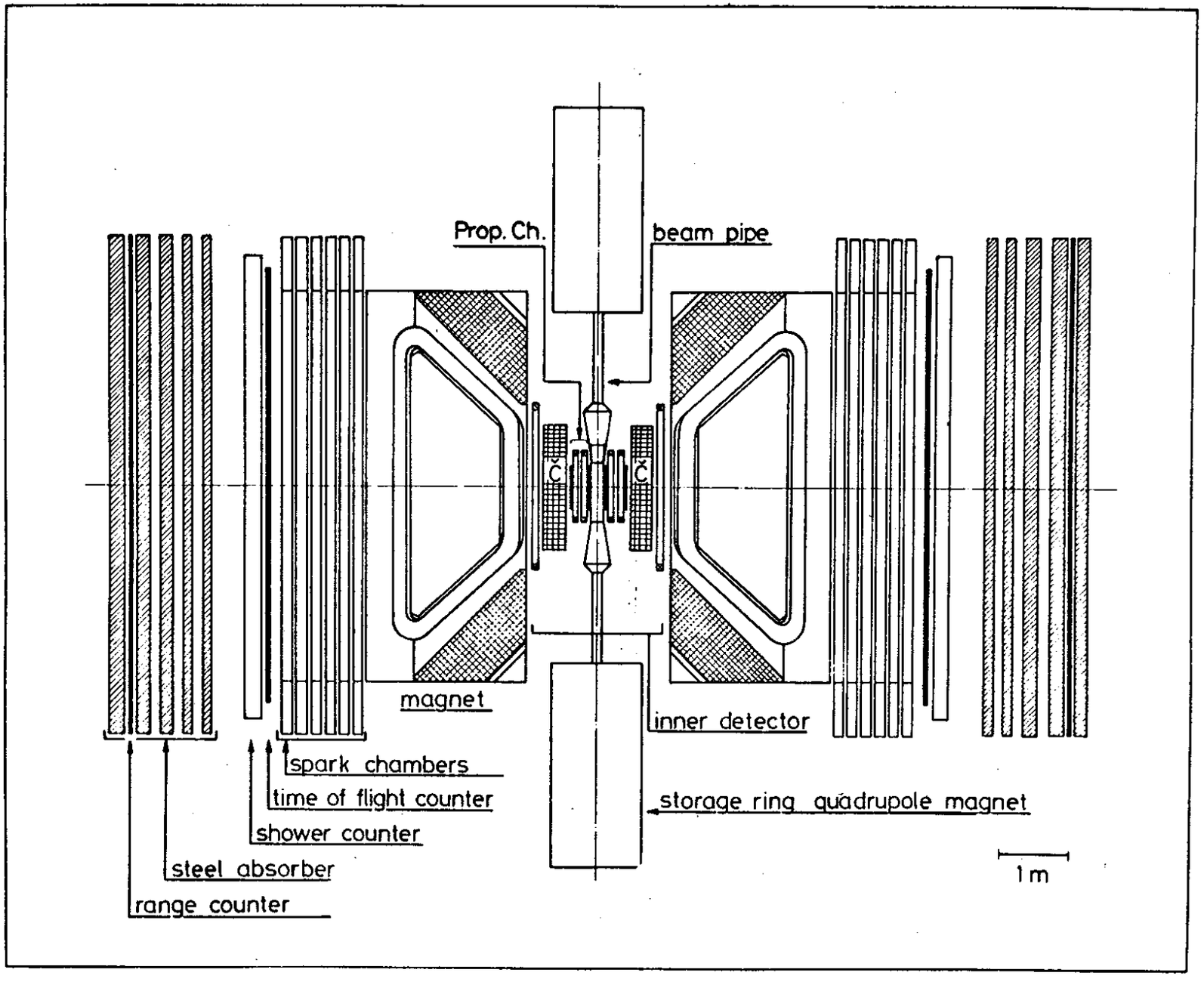
Prop. Ch.
beam pipe
PC
PC
magnet
inner detector
spark chambers
time of flight counter
shower counter
steel absorber
range counter
storage ring quadrupole magnet
1 m

Fig. 1

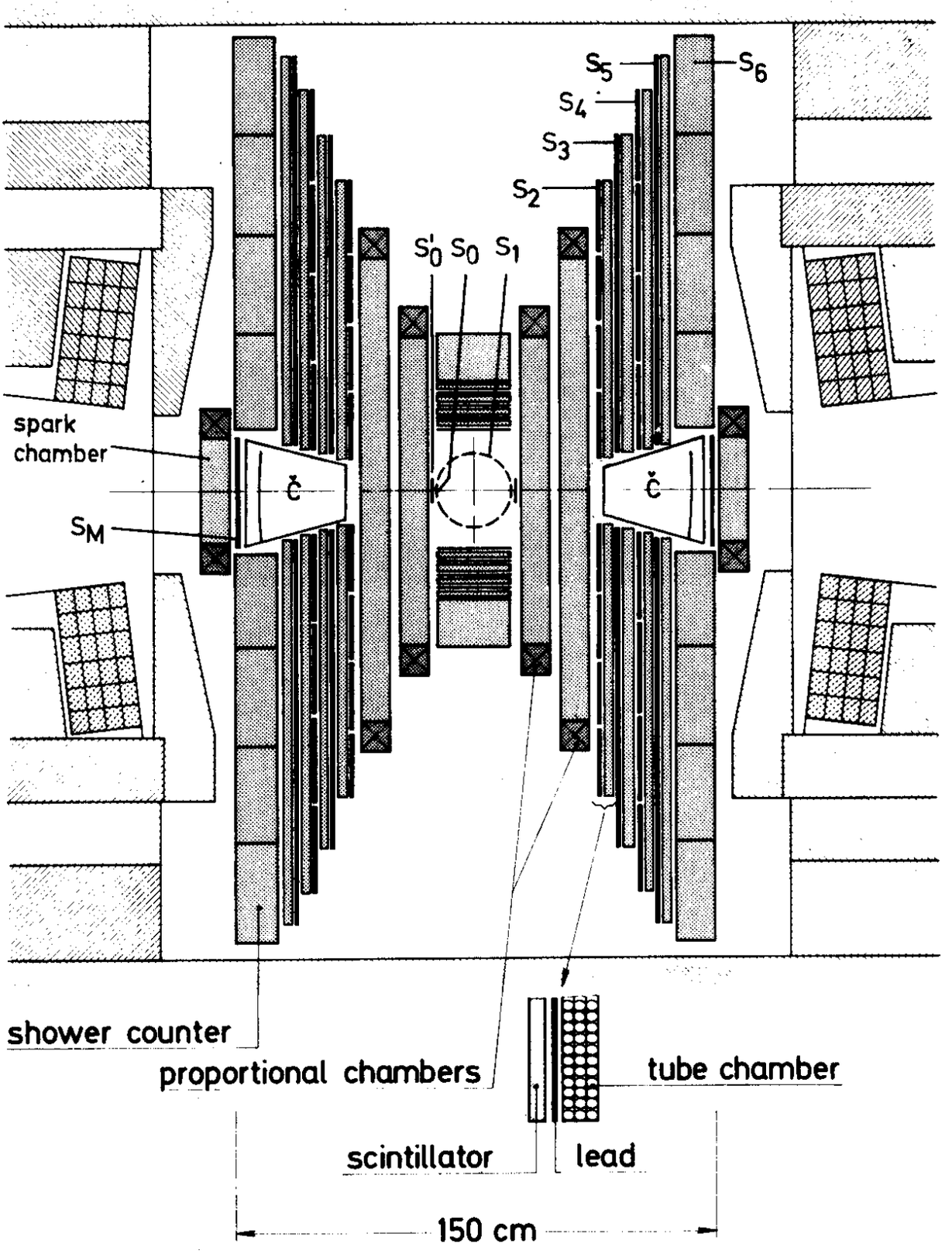
S5
S6
S4
S3
S2
S'0
S0
S1
spark
chamber
Č
Č
SM
shower counter
proportional chambers
tube chamber
scintillator
lead
150 cm

Fig. 2

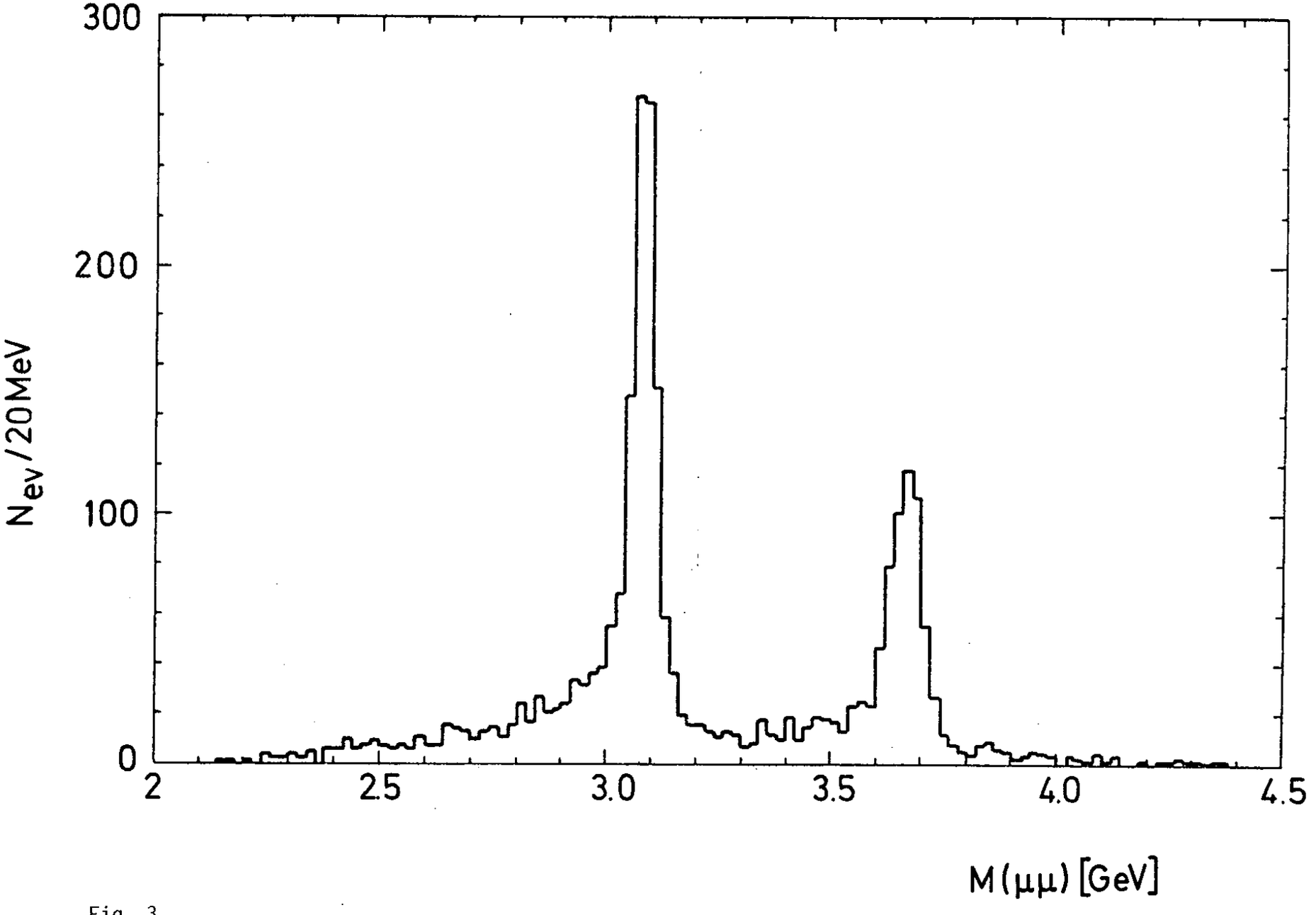

Fig. 3

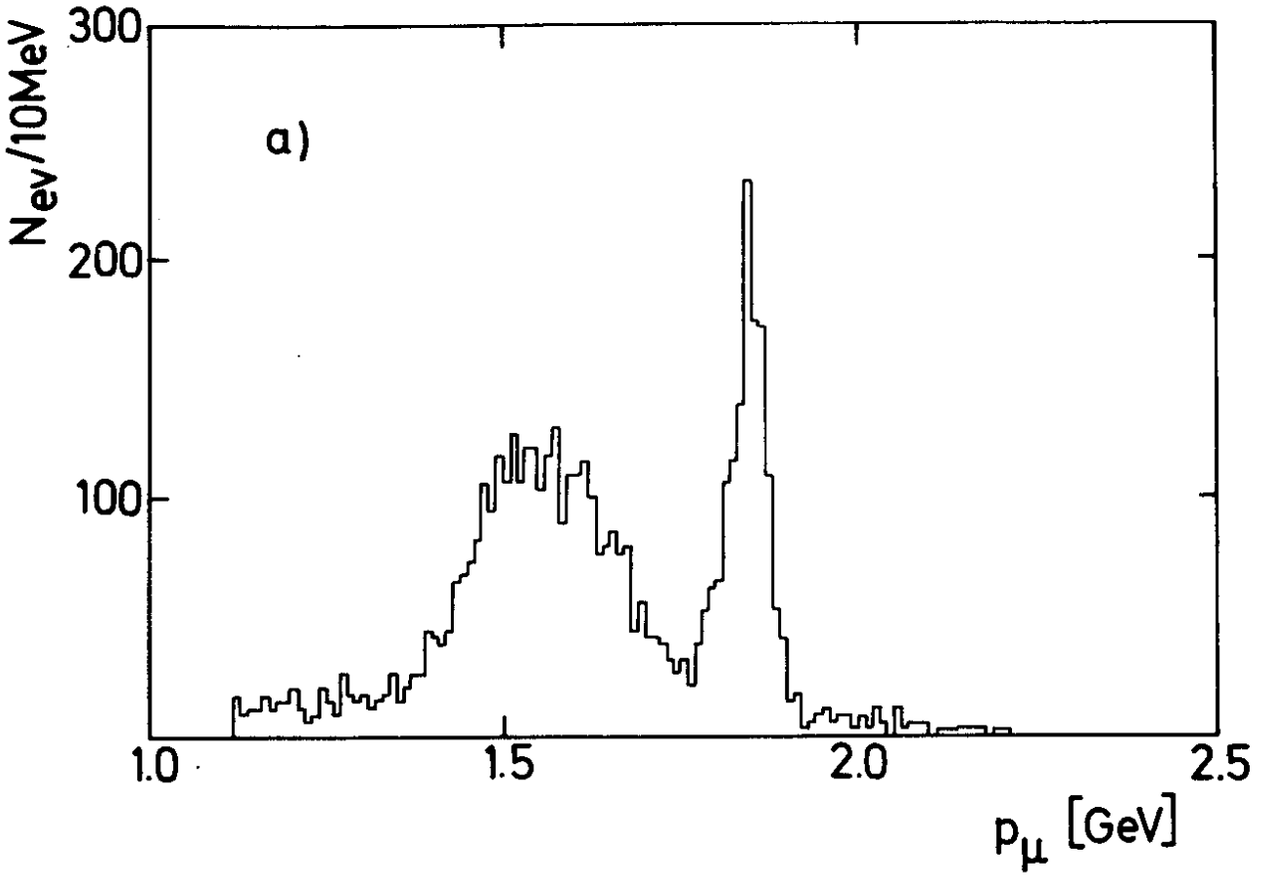
a)
300
200
100
N_{ev}/10MeV
1.0
1.5
2.0
2.5
p_μ [GeV]

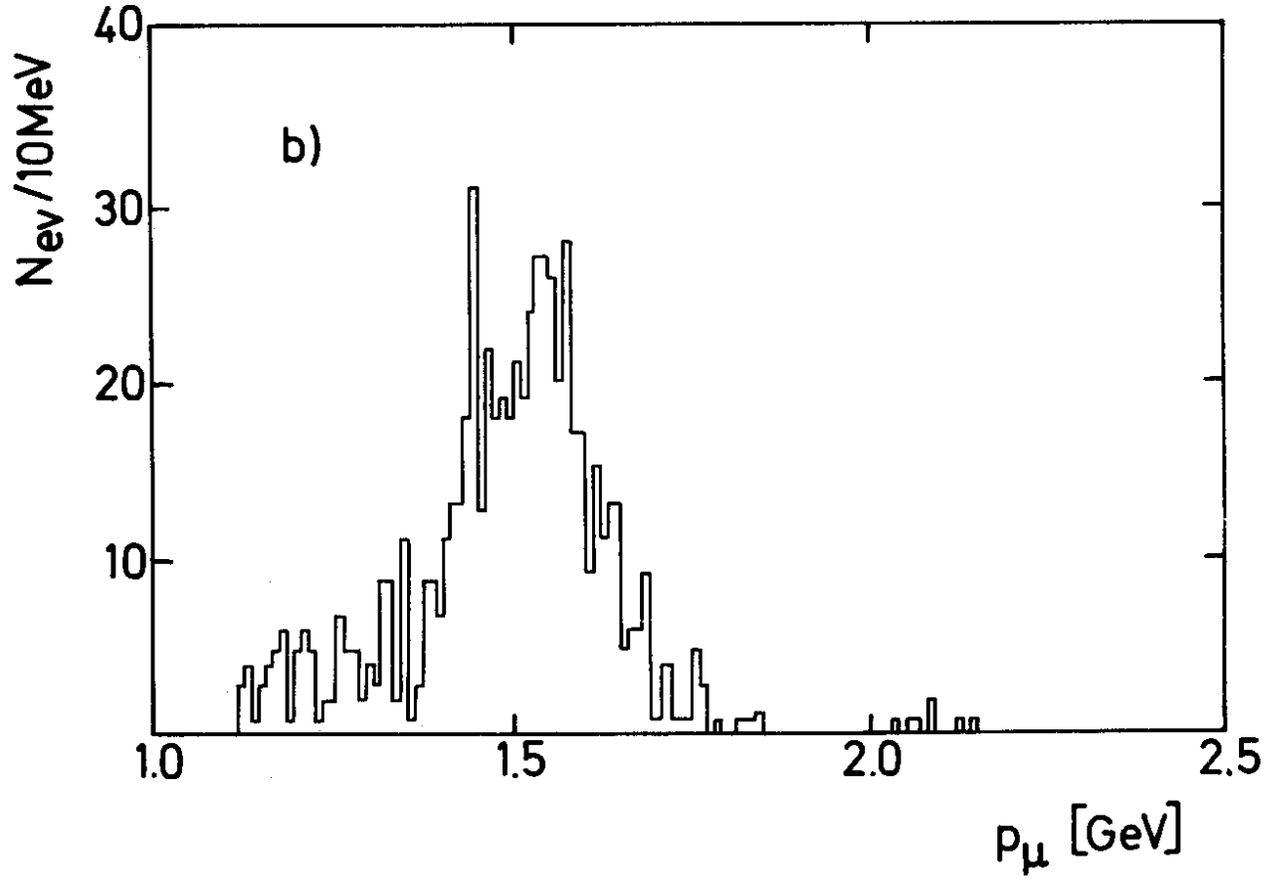
b)
40
30
20
10
N_{ev}/10MeV
1.0
1.5
2.0
2.5
p_μ [GeV]

Fig. 4

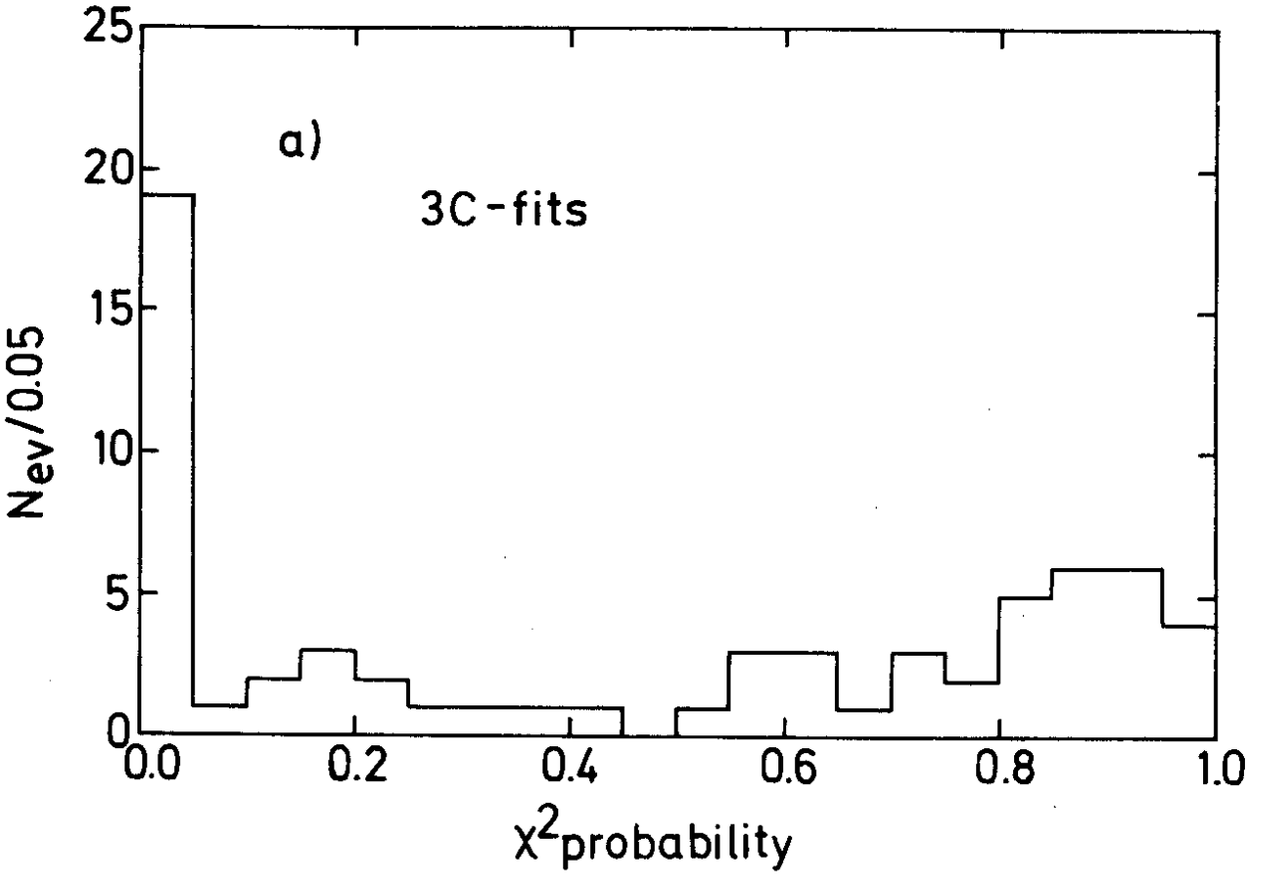
a)
3C-fits
$N_{ev}/0.05$
χ^2probability
0.0
0.2
0.4
0.6
0.8
1.0
0
5
10
15
20
25

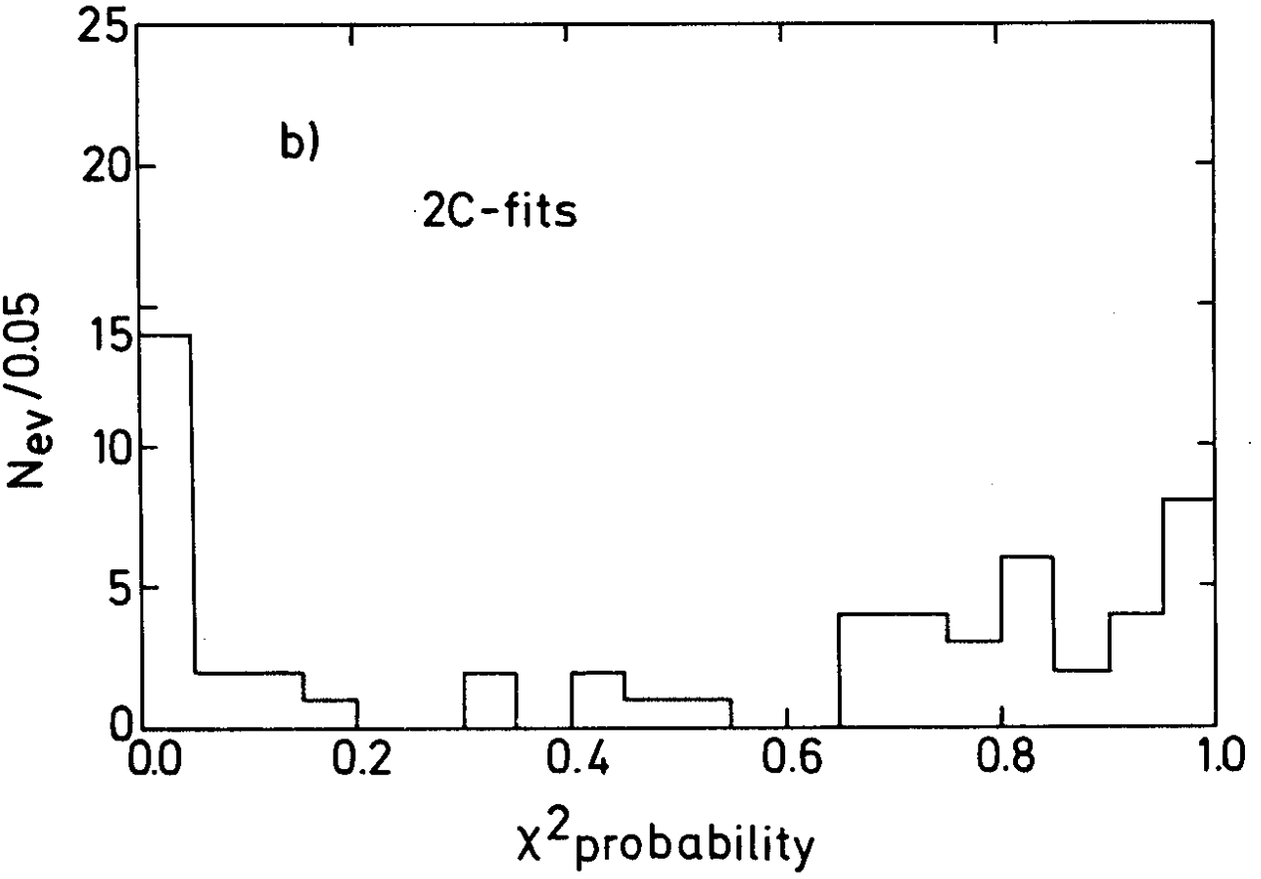
b)
2C-fits
$N_{ev}/0.05$
χ^2probability
0.0
0.2
0.4
0.6
0.8
1.0
0
5
10
15
20
25

Fig. 5

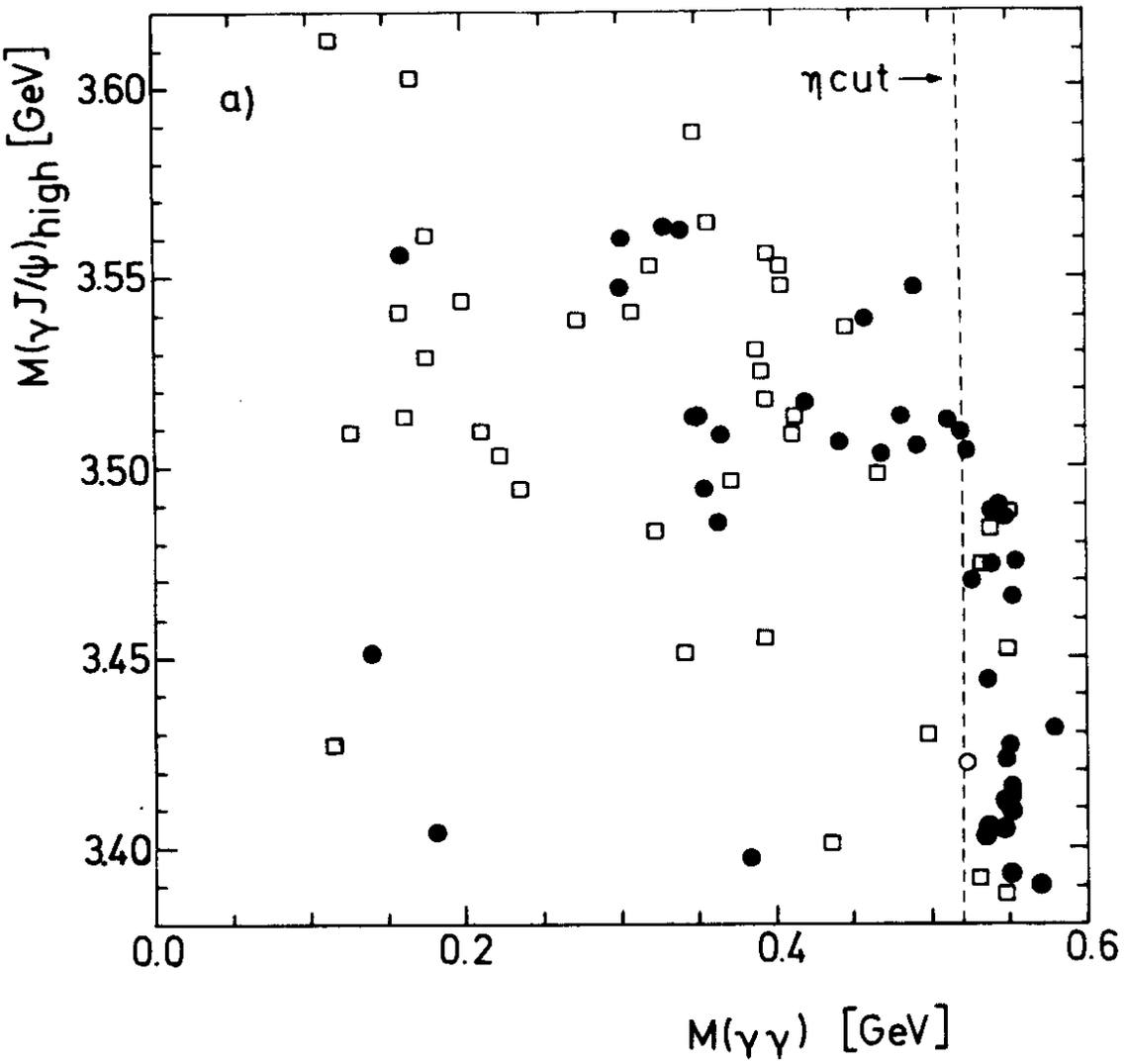
a)
ηcut
M(γJ/ψ)high [GeV]
3.60
3.55
3.50
3.45
3.40
0.0
0.2
0.4
0.6
M(γγ) [GeV]

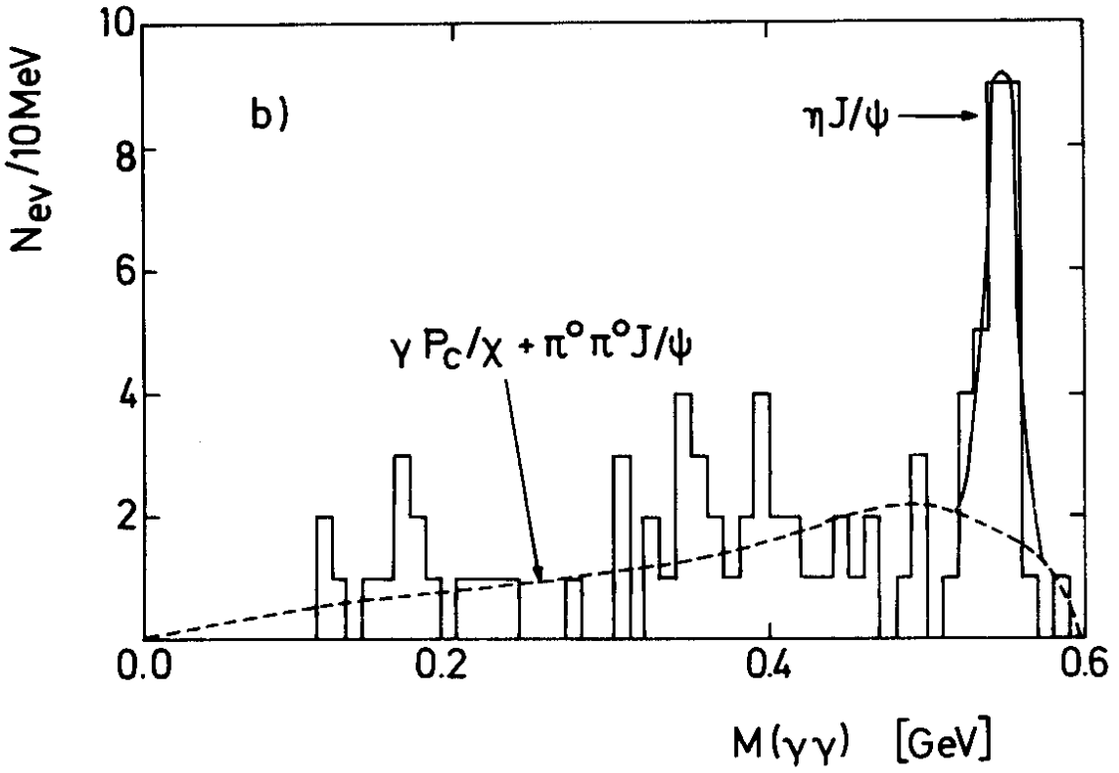
b)
ηJ/ψ
γ Pc/χ + π°π°J/ψ
Nev/10MeV
10
8
6
4
2
0.0
0.2
0.4
0.6
M(γγ) [GeV]

Fig. 6

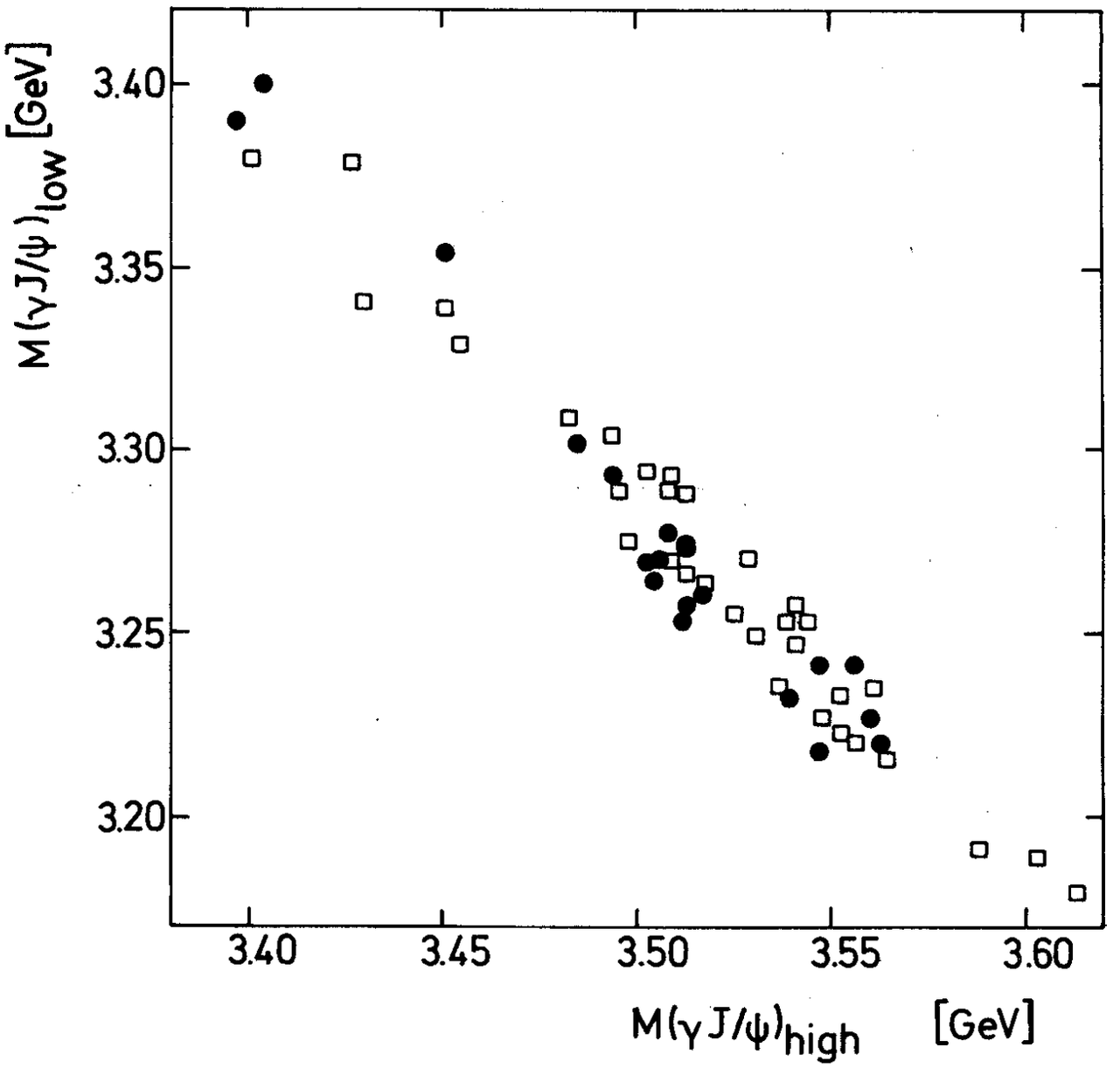
M(γJ/ψ)low [GeV]
3.40
3.35
3.30
3.25
3.20
3.40
3.45
3.50
3.55
3.60
M(γJ/ψ)high [GeV]

Fig. 7

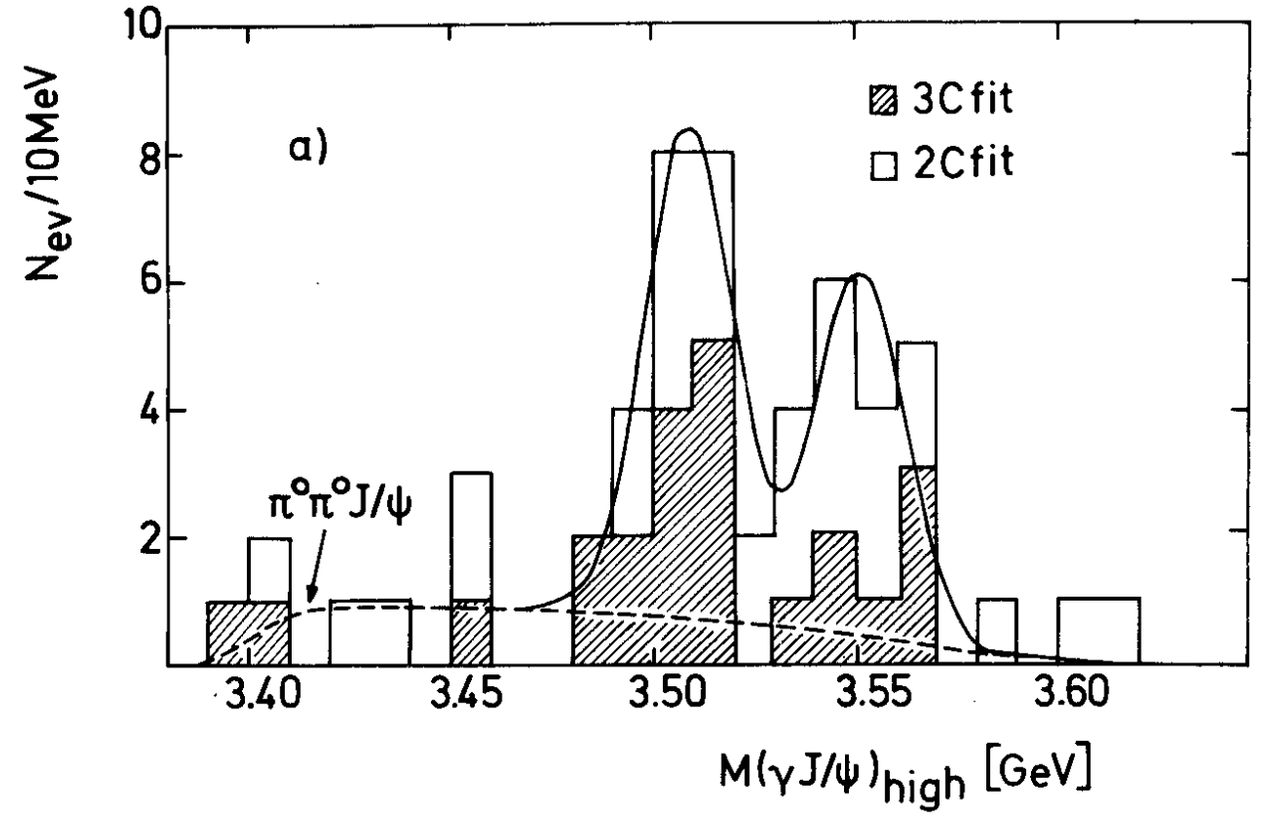
a)
3Cfit
2Cfit
$\pi^0\pi^0 J/\psi$
$N_{ev}/10MeV$
$M(\gamma J/\psi)_{high}$ [GeV]
10
8
6
4
2
3.40
3.45
3.50
3.55
3.60

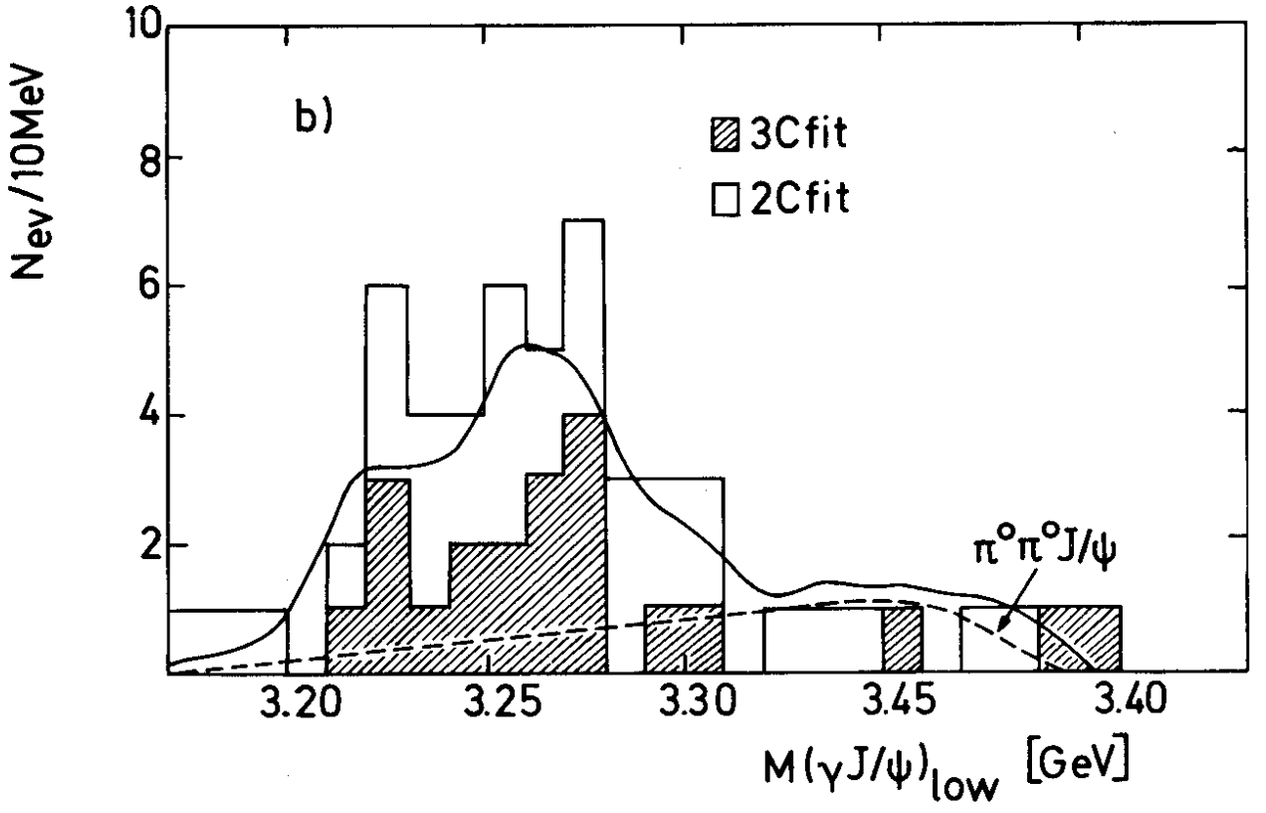
b)
3Cfit
2Cfit
$\pi^0\pi^0 J/\psi$
$N_{ev}/10MeV$
$M(\gamma J/\psi)_{low}$ [GeV]
10
8
6
4
2
3.20
3.25
3.30
3.45
3.40

Fig.8

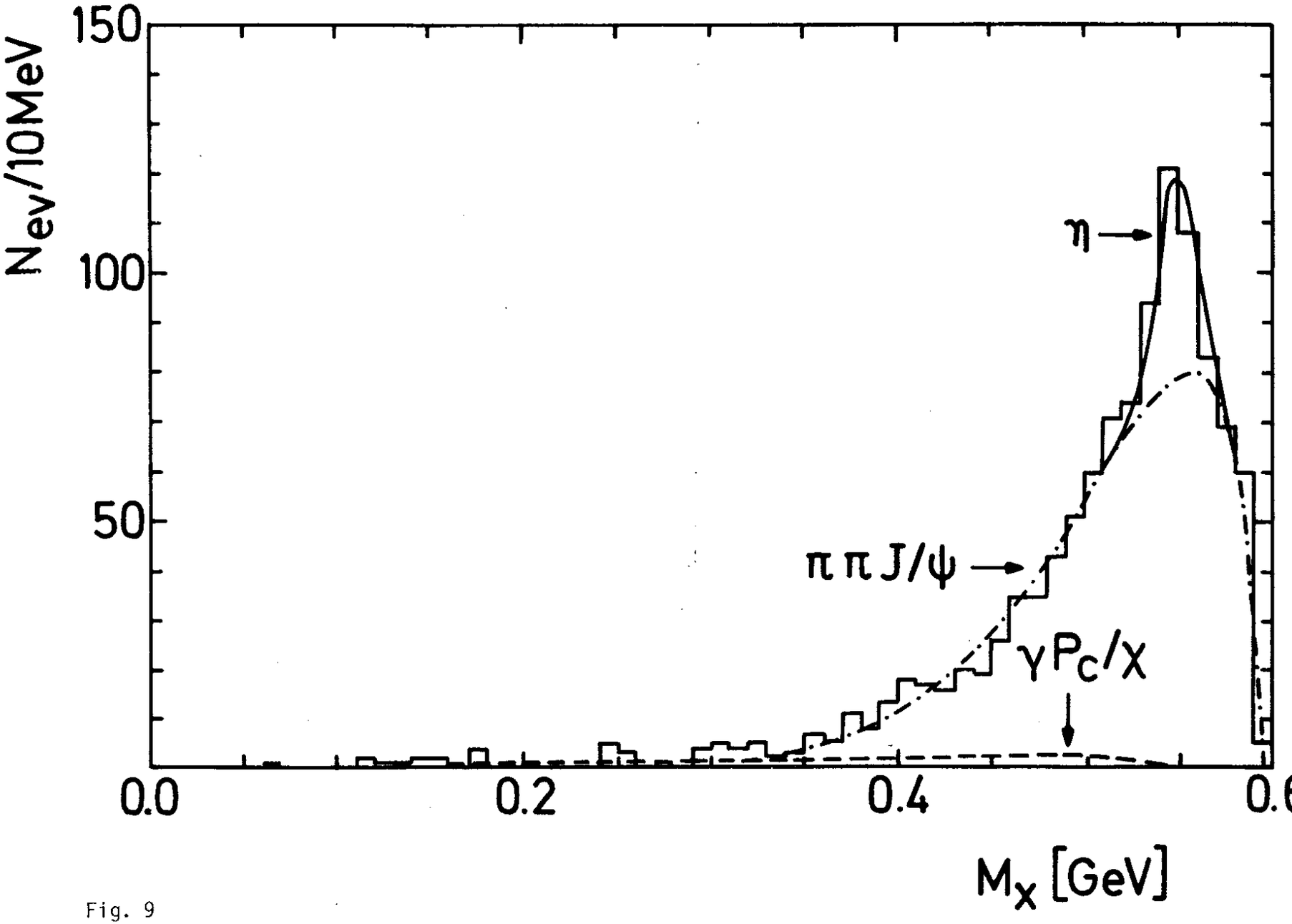

Fig. 9

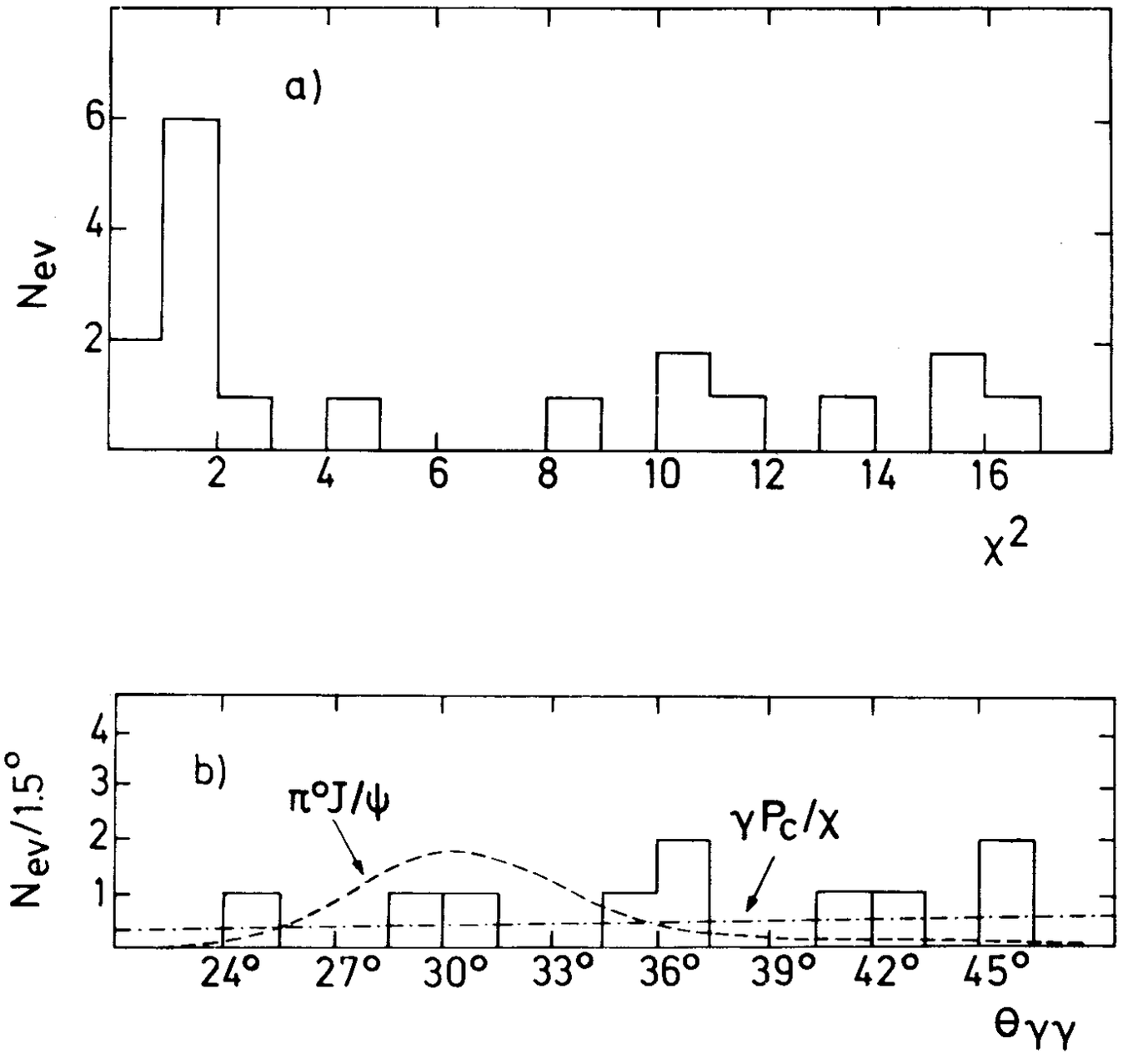
a)
N_{ev}
6
4
2
2
4
6
8
10
12
14
16
χ^2
b)
$\pi^o J/\psi$
$\gamma P_c/\chi$
$N_{ev}/1.5^o$
4
3
2
1
24°
27°
30°
33°
36°
39°
42°
45°
$\theta_{\gamma\gamma}$

Fig. 10

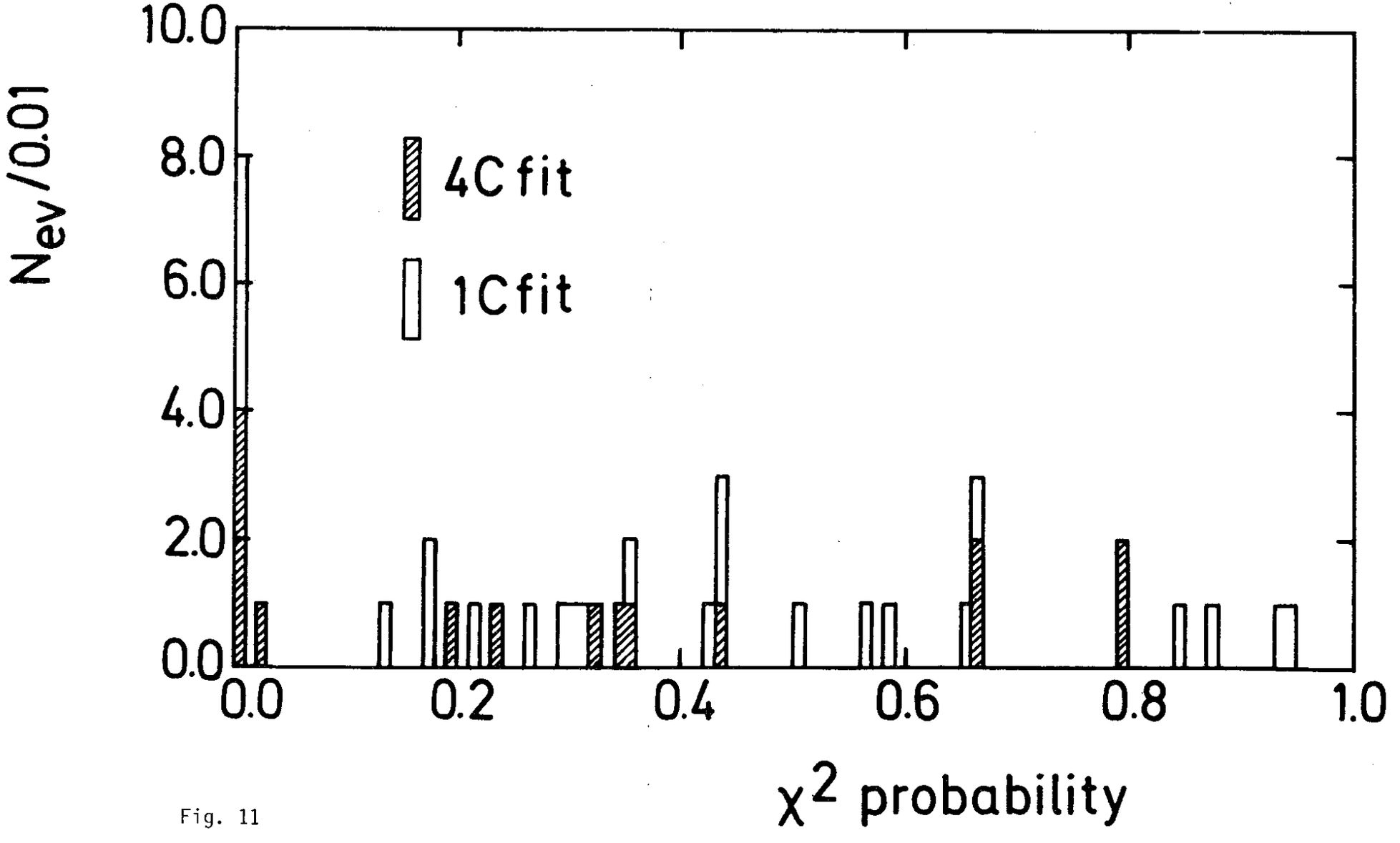
10.0
8.0
6.0
4.0
2.0
0.0
$N_{ev}/0.01$
4C fit
1C fit
0.0
0.2
0.4
0.6
0.8
1.0
χ^2 probability

Fig. 11

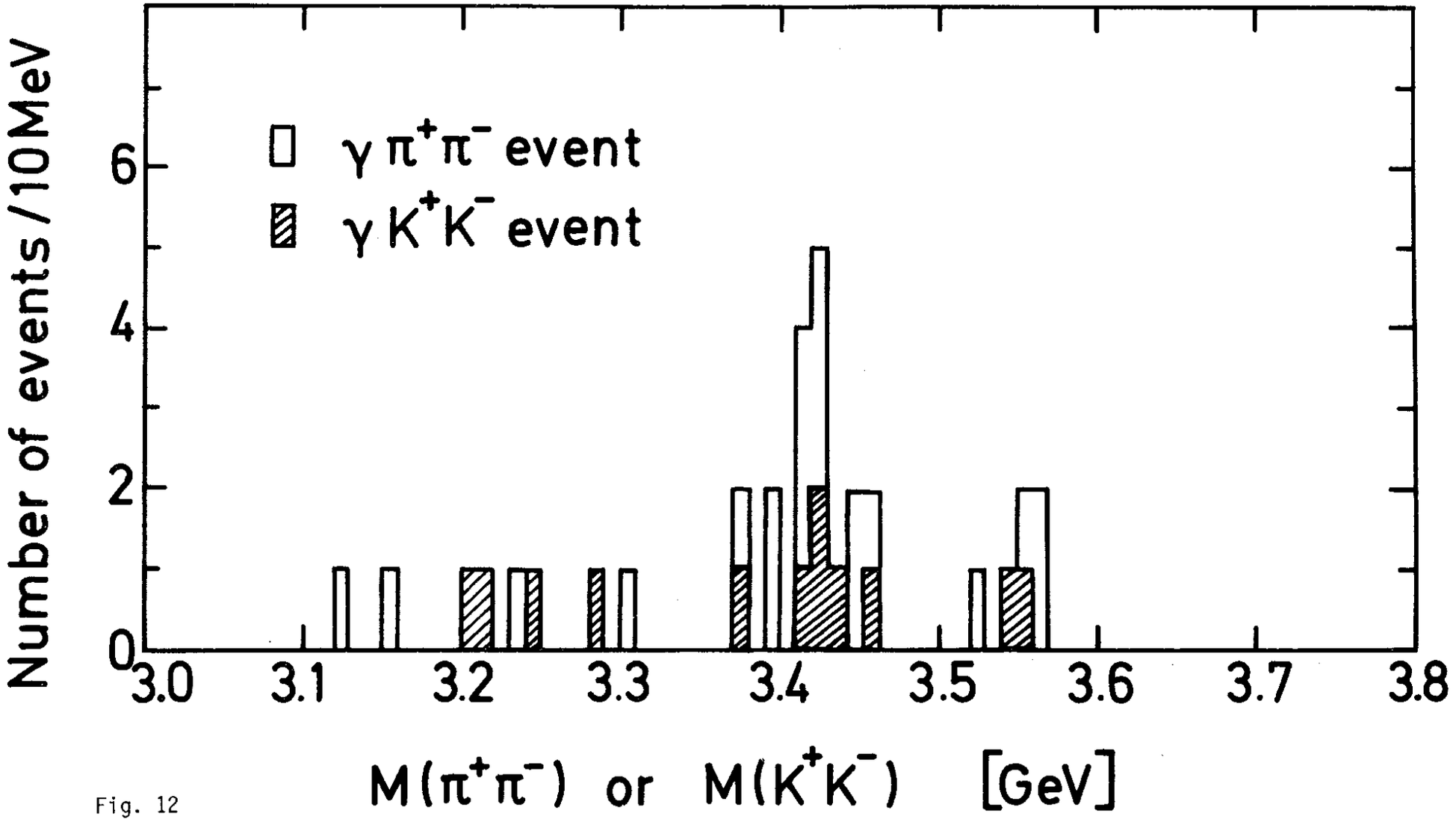
Number of events/10MeV
0
2
4
6
γ π+π− event
γ K+K− event
3.0
3.1
3.2
3.3
3.4
3.5
3.6
3.7
3.8
M(π+π−) or M(K+K−) [GeV]

Fig. 12